

Graphene Oxide Mimics Biological Signaling Cue to Rescue Starving Bacteria

Joshua A. Jackman, Bo Kyeong Yoon, Natalia Mokrzecka, Gurjeet Singh Kohli, Elba R. Valle-González, Xinyi Zhu, Martin Pumera, Scott A. Rice, and Nam-Joon Cho*

There is extensive debate about how 2D nanomaterials such as graphene oxide (GO) affect bacteria. Various effects of GO are proposed, including bacterial growth inhibition or enhancement, killing, and no activity. Herein, we report that GO protects *Staphylococcus aureus* bacterial cells from death in starvation conditions with up to a 1000-fold improvement in cell viability. Transcriptomic profiling reveals that bacterial cells in starvation conditions generally shut down metabolic activity, while only cells incubated with GO increase production of specific enzymes involved in the glyoxalase detoxification pathway along with repressed autolysis. The oxygen-containing functional groups of GO resemble the molecular structure of methylglyoxal, which bacteria produce to adapt to nutrient imbalances and is detoxified by glyoxalase enzymes. The ability of GO to enable bacterial cell survival in starvation conditions and accompanying cellular responses support that bacterial cells perceive GO as a methylglyoxal-mimicking nanomaterial cue to reshuffle cellular metabolism and defenses.

filtration,^[11,12] and sensing.^[13,14] Two-dimensional graphene oxide (GO) sheets are a well-studied nanomaterial example, which have long been observed to kill, inhibit, or enhance the growth of bacteria.^[15–18] More recently, it has been suggested that high-purity GO has no effect on bacteria and chemical impurities related to GO synthesis, not GO itself, are the cause of antibacterial activity.^[19] As such, there is extensive interest in clarifying how 2D nanomaterials such as GO affect bacteria^[20–22] and such insights can guide next-generation nanomaterial design and surface functionalization.

The reactive oxygen-containing functional groups present on the GO sheet surface are presumed to influence biological activities, including bacterial cell interactions.^[23] Specifically, these functional groups are implicated in GO-mediated

oxidative stress, which occurs when a biological system is unable to cope with the quantity of reactive oxygen species (ROS) that is being produced.^[24] Excessive oxidative stress can lead to deleterious outcomes such as impaired cell function or death, while bacterial pathogens such as *Staphylococcus aureus* (*S. aureus*) have evolved the ability to withstand high levels of

1. Introduction

The interaction of bacteria with nanomaterials is relevant to various health and environmental issues such as bacteria killing,^[1–3] antifouling surfaces,^[4–6] antibacterial drug resistance,^[7] microbial ecology,^[8,9] bio-recycling,^[10] water

Prof. J. A. Jackman, Dr. B. K. Yoon, N. Mokrzecka, E. R. Valle-González, Prof. N.-J. Cho

School of Materials Science and Engineering
Nanyang Technological University
Singapore 639798, Singapore
E-mail: njcho@ntu.edu.sg

Prof. J. A. Jackman, Dr. B. K. Yoon
School of Chemical Engineering and Biomedical Institute for
Convergence at SKKU (BICS)
Sungkyunkwan University
Suwon 16419, Republic of Korea

Dr. G. S. Kohli, Dr. X. Zhu, Prof. S. A. Rice, Prof. N.-J. Cho
Singapore Centre for Environmental Life Sciences Engineering
Singapore 637551, Singapore

Prof. M. Pumera
Future Energy and Innovation Lab
Central European Institute of Technology
Brno University of Technology
Brno 61600, Czech Republic

 The ORCID identification number(s) for the author(s) of this article can be found under <https://doi.org/10.1002/adfm.202102328>.

Prof. M. Pumera
3D Printing and Innovation Hub
Department of Chemistry and Biochemistry
Mendel University in Brno
Zemědělska 1, Brno CZ-61300, Czech Republic

Prof. M. Pumera
Department of Medical Research
China Medical University Hospital
China Medical University
Taichung 40402, Taiwan

Prof. M. Pumera
Department of Chemical and Biomolecular Engineering
Yonsei University
Seoul 03722, Republic of Korea

Prof. S. A. Rice
School of Biological Sciences
Nanyang Technological University
Singapore 637551, Singapore

Prof. S. A. Rice
ithree Institute
University of Technology Sydney
Ultimo, New South Wales 2007, Australia

DOI: 10.1002/adfm.202102328

oxidative stress.^[25] To evade oxidative damage, *S. aureus* has developed various strategies for cellular protection, detoxification, and repair.^[26] Such capabilities help to explain why *S. aureus* is a leading cause of human infections worldwide, especially with its ability to overcome host cellular defenses involving the release of reactive oxygen and nitrogen species.^[27,28]

Since *S. aureus* elicits distinct cellular responses depending on the chemical source of oxidative stress,^[29,30] we sought to investigate how *S. aureus* bacterial cells in nutrient-limiting starvation conditions respond to oxidative stress-inducing GO sheets. In addition to determining the empirical effect of GO on *S. aureus* bacterial cells in starvation conditions, we sought to unravel the molecular mechanisms behind cellular responses.

2. Results and Discussion

Current models of how bacterial cells interact with GO nanomaterials are presented in **Figure 1a** and our experimental strategy to characterize the interactions between oxidative stress-inducing GO sheets and *S. aureus* bacterial cells, involved

a combination of nanomaterial characterization, microbiological testing, and transcriptomic analyses (RNA-seq) (**Figure 1b**).

We fabricated GO sheets with varying degrees of oxidizing activity according to the 1) Staudenmaier, 2) Hoffman, 3) Hummers, and 4) Tour methods, as previously described.^[31] The Staudenmaier and Hoffman methods involve chlorate oxidants that result in a higher carbon/oxygen (C/O) atomic ratio and mainly hydroxyl and epoxy functional groups on the GO sheet surface while the Hummers and Tour methods involve permanganate oxidants that yield a smaller C/O ratio and a greater density of carbonyl and carboxylic acid functional groups. The GO sheets were extensively rinsed with water until neutralized and are referred to as GO samples 1–4 according to the preparation methods listed above. Aqueous dispersibility of the GO samples was observed and is consistent with hydrophilic surface properties due to the presence of oxygen-containing functional groups, which led us to evaluate pertinent solution-phase behaviors.

The in vitro oxidizing activity of the solution-phase GO samples was first characterized by measuring the extent to which GO can convert glutathione (GSH), an important tripeptide antioxidant that helps *S. aureus* cope with ROS,^[32] into

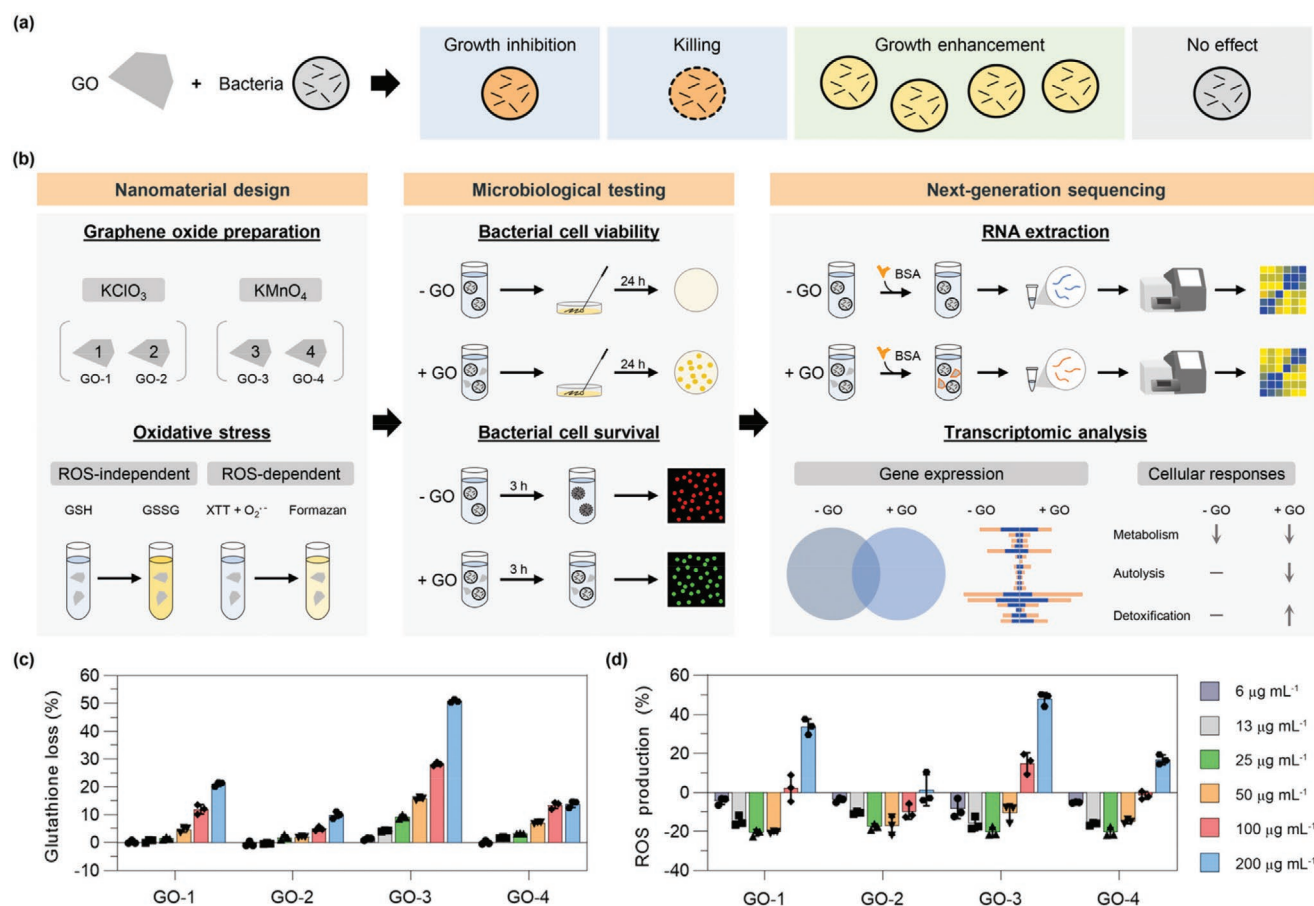


Figure 1. Experimental strategy and characterization of GO-mediated oxidative stress. a) Current models of GO nanomaterial interactions with bacteria. b) Illustration of the experimental concept to characterize GO interactions with *S. aureus* bacterial cells under starvation conditions. Effect of GO on c) glutathione loss and d) superoxide radical anion ROS production. A twofold dilution series of GO samples with 6–200 $\mu\text{g mL}^{-1}$ concentrations were incubated in aqueous solution with reagents for 3 h, followed by measurement. The data are presented in percentage units relative to negative control experiments without GO. Results in (c) and (d) are expressed as mean \pm standard deviation (s.d.) ($n = 3$ biological replicates).

glutathione disulfide (GSSG) (Figure 1c). Greater GSH consumption is associated with more oxidizing activity. GO samples ($6\text{--}200\ \mu\text{g mL}^{-1}$) were incubated with GSH and UV-vis spectroscopy experiments revealed dose-dependent oxidation in all cases. At the highest GO concentration of $200\ \mu\text{g mL}^{-1}$, sample 3 caused 51% GSH oxidation while samples 1, 2, and 4 caused 21%, 10%, and 14% GSH oxidation, respectively. We also measured the GO-mediated production level of superoxide radical anion, which is an ROS involved in oxidative stress (Figure 1d). Low concentrations of GO, up to $25\ \mu\text{g mL}^{-1}$, tended to decrease superoxide radical anion production by around 20%, while higher concentrations of GO caused dose-dependent increases in production compared to the baseline. At $200\ \mu\text{g mL}^{-1}$ GO, sample 3 caused the highest production levels with around a 57% increase while samples 1, 2, and 4 increased production levels by around 42%, 7%, and 24%, respectively. The trends across both experiments were consistent and support that GO samples caused dose-dependent oxidative stress to varying extents while low GO concentrations partially suppressed superoxide radical anion production.

In nutrient-limiting conditions, *S. aureus* bacterial cells experience stress and lose viability over time.^[33] The extent of viability loss depends on the environment, and cells become nonculturable in the absence of amino acids or phosphate. We initially tested the time-dependent viability of *S. aureus* cells that were suspended in 10 mM phosphate buffer (PB) at a density of $\approx 5.5 \times 10^5$ colony-forming units per mL (CFU mL^{-1}). Viable counts were determined by plating the treated cells on Mueller-Hinton (MH) agar plates overnight, followed by CFU

enumeration (Figure 2a; Figure S1, Supporting Information). After 1 h incubation, the number of viable cells decreased by more than 87% and there was a >99% loss in viable cells after 2 h incubation. Accordingly, GO samples were dispersed in PB solution at a concentration of 50 or $200\ \mu\text{g mL}^{-1}$, and *S. aureus* cells were suspended in the GO-containing PB solution for 3 h before plating. For all samples, the presence of GO led to a marked increase in the number of viable cells and GO protected against viability loss in a dose-dependent manner (Figure 2b). At $200\ \mu\text{g mL}^{-1}$ GO, sample 3 preserved around 80% bacterial cell viability compared to the initial inoculum while samples 1, 2, and 4 maintained viability levels around 57%, 36%, and 56%, respectively. Thus, GO protected *S. aureus* cell viability in nutrient-limiting conditions by over 1000-fold and the degree of cellular protection mirrored the trend in GO oxidizing capacity.

To verify if GO aids bacterial cell survival, *S. aureus* cells (density of 1×10^7 CFU mL^{-1}) were incubated for 3 h with $200\ \mu\text{g mL}^{-1}$ GO in PB solution or phosphate-buffered saline (PBS), and the percentage of live and dead bacterial cells was determined by fluorescence microscopy (Figure 2c). Live and dead bacterial cells are indicated by green and red colors, respectively. Over the incubation period, the percentage of live cells in PB solution decreased from 97% to 33%, while GO had significant protective effects, as indicated by 89% survival (Figure 2d). By contrast, the percentage of live cells before and after incubation in PBS was nearly equivalent ($\approx 95\%$), and GO neither increased nor decreased bacterial cell viability, which agrees with past observations.^[19] In both PB and PBS conditions, the microscopy images also showed that GO-treated

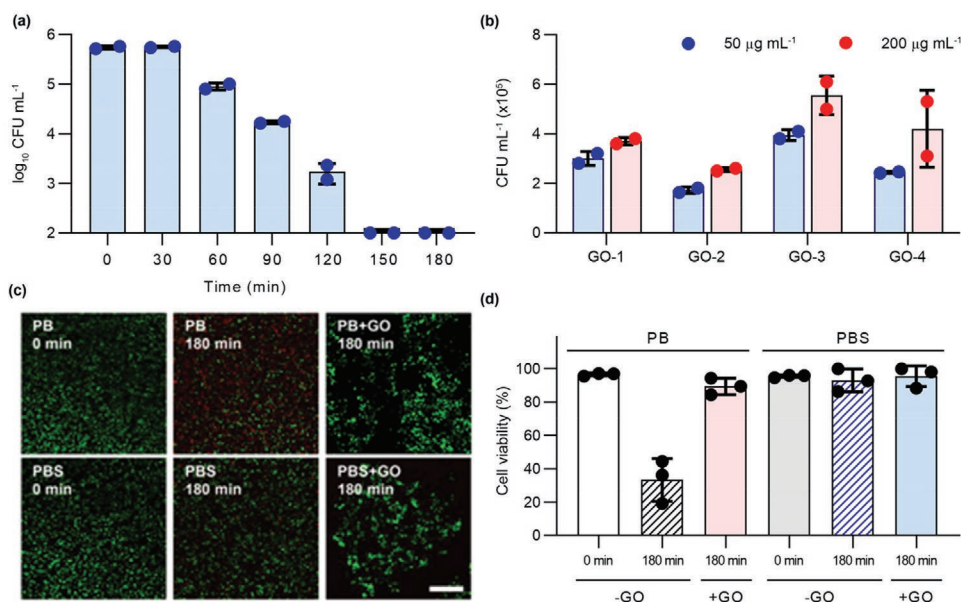


Figure 2. GO-mediated protection of starving *S. aureus* bacterial cells. a) Time-dependent viability of *S. aureus* cells suspended in phosphate buffer (PB) solution without GO. Cells at a density of 5.5×10^5 CFU mL^{-1} were incubated for up to 3 h and cell viability was determined every 30 min by agar plating and colony-forming unit (CFU) enumeration ($n = 2$ biological replicates). b) Effect of GO on *S. aureus* cell viability in PB solution. *S. aureus* cells at a density of 5.9×10^5 CFU mL^{-1} were incubated for 3 h in PB solution together with 50 or $200\ \mu\text{g mL}^{-1}$ GO. Cell viability was determined by agar plating and CFU enumeration ($n = 2$ biological replicates). Results in (a) and (b) are expressed as mean \pm s.d. c) Fluorescence microscopy images of *S. aureus* cells before and after 3 h incubation in PB or phosphate-buffered saline (PBS) solutions. *S. aureus* cells at a density of 1×10^7 CFU mL^{-1} were incubated alone or together with $200\ \mu\text{g mL}^{-1}$ GO. Scale bar, 100 μm . Green, SYTO 9 dye; red, propidium iodide dye. The images are representative of two independent experiments. d) Percentage of live *S. aureus* cells based on fluorescence microscopy quantification ($n = 3$ biological replicates). Results are expressed as mean \pm standard error of the mean (s.e.m.).

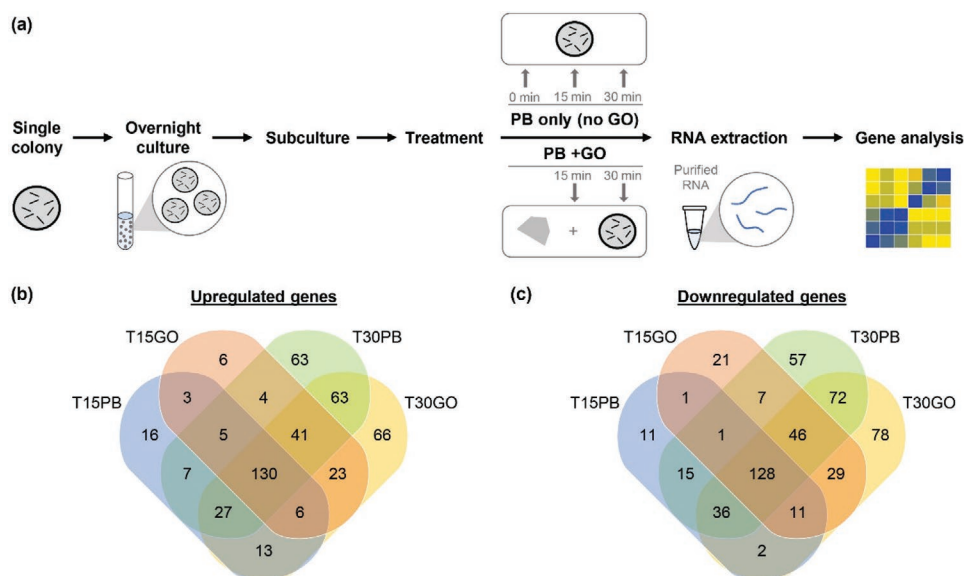


Figure 3. Transcriptomic profiling of starving *S. aureus* bacterial cells and GO effects. a) Experimental strategy for RNA-seq analysis of *S. aureus* bacterial cell responses in starvation conditions consisting of phosphate buffer (PB) solution. PB and PB+GO denote bacterial samples without and with GO, respectively. The bacterial samples were incubated in the PB solution for 15 or 30 min, along with a control sample without incubation (0 min). Venn diagrams for number of genes at least twofold b) upregulated and c) downregulated for bacterial samples in different conditions compared to the control sample. T15PB and T30PB refer to bacterial samples without GO after 15- and 30-min incubation, respectively. T15GO and T30GO refer to bacterial samples with GO after 15- and 30-min incubation, respectively.

bacteria appeared to coalesce, which supports that adhesive interactions between bacterial cells and hydrophilic GO sheets contribute to the observed protective effects. Taken together, the findings establish that GO protected against cell death in nutrient-limiting solution conditions in the absence of salts.

To decipher the molecular basis for GO-induced bacterial cell protection, transcriptomic profiling was conducted^[34] and we measured RNA expression levels of *S. aureus* bacterial cells incubated in PB in the presence and absence of GO (labeled as PB+GO and PB, respectively). *S. aureus* cells (density of $\approx 6 \times 10^8$ CFU mL⁻¹) were incubated with GO (400 μ g mL⁻¹) for 15 or 30 min, and equivalent control experiments were performed without GO (Figure 3a; Figures S2 and S3, Supporting Information). These time points were chosen because there was not a significant loss in cell viability up to 30 min, while the cells resuspended in PB showed >80% loss in cell viability by 60 min. After incubation, the cell-GO samples were treated with bovine serum albumin (BSA) protein to passivate the GO surface^[35] before adding lysostaphin enzyme to digest *S. aureus* cell walls, liberating cellular RNA which was collected for deep-sequencing analysis. The BSA passivation step minimized RNA attachment to the GO surface upon intracellular RNA release and hence facilitated efficient RNA extraction, which was otherwise encumbered by strong GO-RNA binding interactions (Note S1 and Figure S4, Supporting Information). To determine if there was a difference in the expression of stress-related genes for PB and PB+GO treated cultures, we quantified genome-wide differences in transcription at the different time points. Based on global analysis, 258 (130 upregulated and 128 downregulated) genes were similarly altered in expression for both the PB and PB+GO samples (Figure 3b,c).

Genes associated with genetic information processing, such as those involved in translation and ribosome expression, were generally reduced in expression for all conditions (Figure 4a). Similarly, genes involved in glycolysis, the RNA polymerase subunit delta (ID 14075), and the cell division protein ftsW (ID 09520) were strongly repressed, suggesting a general shut-down of cellular metabolism in response to stress conditions. To better understand changes in gene expression that might explain the increased survival of PB+GO treated bacterial cells, we focused on genes that were differentially expressed between the two conditions, relative to the initial culture. At 15 and 30 min, 462 (218 upregulated and 244 downregulated) and 771 (369 upregulated and 402 downregulated) genes were differentially expressed in the PB+GO condition (Data S1, Supporting Information).

One of the most highly induced genes in the PB+GO treated cultures was a putative glyoxalase enzyme (gene number 13170) that was induced 10- and 13-fold after 15 and 30 min, respectively (Figure 4b). Similarly, 13165, which is adjacent to, and may be co-transcribed with, the glyoxalase gene, was induced 15- to 17-fold in the presence of PB+GO. This gene is annotated as a putative carboxylesterase and has no known function, but its similarly high induction in the presence of GO suggests it may work in conjunction with the putative glyoxalase. In marked contrast, neither of these genes was differently expressed in the PB condition and the 13170 and 13165 genes were induced by seven- and eightfold, respectively, in the PB+GO condition at 15 min. Three additional genes in the *S. aureus* genome were annotated as glyoxalases (01465, 07875, and 13185). Two of these, 13185 and 07875, were similarly repressed under both conditions while 01465 was also induced in the PB+GO condition. Moreover, none of the glyoxalases was induced in the PB condition.

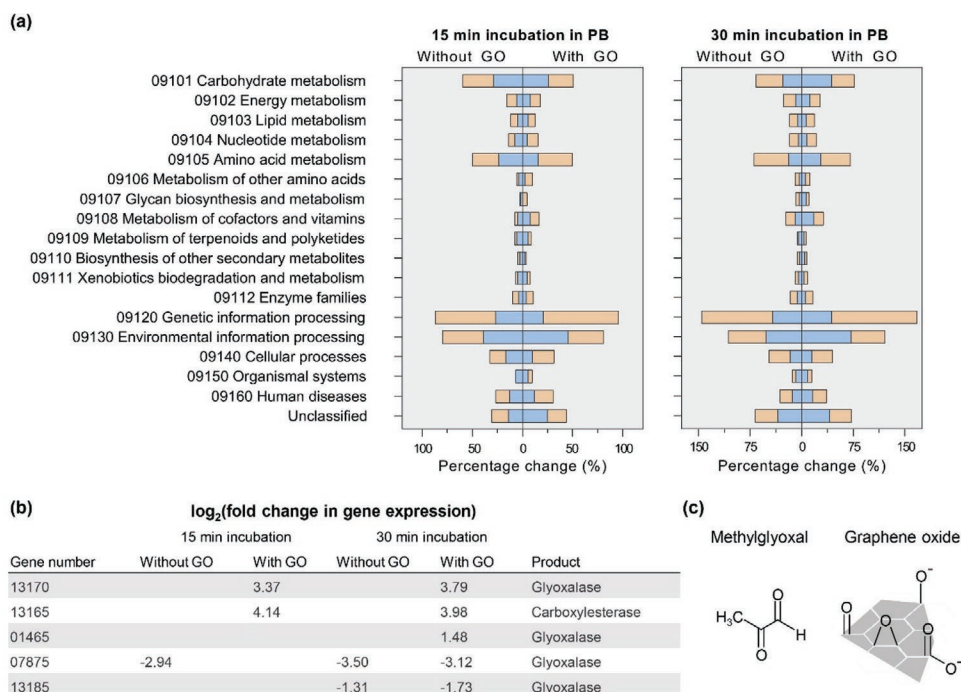


Figure 4. GO triggers specific survival responses associated with methylglyoxal detoxification. a) Distribution of upregulated and downregulated gene transcripts in different conditions according to functional class. The classes were organized based on the KEGG pathway maps. Each bar summarizes the percentage of upregulated (blue) and downregulated (light orange) genes in each category. b) Summary of differentially regulated genes related to the glyoxalase detoxification pathway. The $\log_2(\text{fold-change})$ values are reported for genes with at least twofold significant changes compared to the negative control. Positive and negative values indicate upregulated and downregulated genes, respectively (see also Data S1, Supporting Information). c) Molecular structures of MG and GO functional groups.

In general, genes associated with cell wall synthesis were also repressed in the presence of GO, for example, phage infection protein, sortase, *lysM*, *n*-acetylmuramoyl-*l*-alanine amidase, and *dltA*, suggesting that PB+GO induces cell replication arrest, which may protect the cells from lysis. *nrdR* was also reduced in expression in the PB+GO incubated cells and is a repressor of genes associated with the generation of deoxyribonucleotides from ribonucleotides and may indicate that the PB+GO treated cells are reorganizing metabolism to ensure a proper balance of nucleotides. Together, the data support that PB+GO induces a general shutdown of growth and autolysis in *S. aureus* cells along with inducing a glyoxalase detoxification pathway.

Glyoxalase enzymes are involved in the detoxification of methylglyoxal (MG), which is produced as part of glucose metabolism when bacteria experience nutrient imbalances and need to reshuffle metabolic activities to survive in harsh environmental conditions.^[36] MG production is viewed as a high-risk strategy to facilitate bacterial adaptation because high MG concentrations are associated with DNA damage, mutation, and cell death.^[37] As such, bacterial cells produce glyoxalases in order to convert MG and other reactive aldehydes into less toxic by-products. It is thus striking that the PB+GO condition induces markedly enhanced levels of specific glyoxalase enzymes whereas no such effect is observed in the PB condition only. While MG can be produced endogenously, it can also be added exogenously and trigger chemically induced bacterial cell stress extracellularly.^[38] The toxicity

elicited by MG is related to its molecular structure, which contains two reactive carbonyl groups that exhibit oxidizing activity, including ROS generation, and contribute to oxidative stress^[39] (Figure 4c). The oxygen-containing functional groups of GO resemble the molecular structure of MG and also have similar types of oxidizing activity. Together with the observed induction of the glyoxalase detoxification pathway, these findings support that *S. aureus* bacterial cells perceive GO as an MG-mimicking nanomaterial cue to reshuffle cell metabolism and defenses in a manner that enables bacterial cell survival in otherwise-lethal starvation conditions. While the PBS condition also lacked essential nutrients, our findings show that *S. aureus* bacterial cells remain alive for up to 3 h in that condition. The rapid loss of bacterial cell viability in the PB condition points to the importance of both nutrient limitations and osmolarity-related effects due to the absence of salts. In this latter respect, the GO-induced repression of autolysis genes—which encodes autolytic enzymes that hydrolyze specific linkages within the peptidoglycan cell wall^[40,41]—likely also drives enhanced survival.

3. Conclusion

In summary, our findings demonstrate that GO can enable *S. aureus* bacterial cells to survive in starvation conditions and that the structural and functional properties of oxygen-containing functional groups on the GO sheet surface play

an important role in enabling this protective activity. While oxidative stress is typically associated with harmful effects, there is precedent that an oxidative stress response can help other microorganisms such as yeast survive in starvation conditions.^[42] ROS-mediated oxidative stress elicited by host cell immune responses has also been shown to induce antibiotic tolerance of *S. aureus* bacterial cells.^[30] Our study presents the first example of how a nanomaterial can induce an oxidative stress-related response in living cells—in this case triggered by how *S. aureus* bacterial cells perceive GO as an MG-mimicking cue—that enhances cellular function to survive in starvation conditions. These findings expand on the current knowledge about nanomaterial–cell interactions and demonstrate how nanomaterial-induced oxidative stress can aid, rather than harm, bacterial cells in certain situations. Since many types of Gram-positive and Gram-negative bacteria have glyoxalase enzymes,^[43] it would be interesting to explore the potential effects of GO on a wider range of bacteria in starvation conditions. Looking forward, these results and the methodologies developed in this study open the door to exploring how the wide range of nanomaterials with reactive oxygen-containing functional groups, which are commonly associated with antibacterial mechanisms, might also enhance the function of bacterial cells and other cell types.

Supporting Information

Supporting Information is available from the Wiley Online Library or from the author.

Acknowledgements

J.A.J. and B.K.Y. contributed equally to this work. This work was supported by the National Research Foundation of Singapore through a Competitive Research Programme grant (NRF-CRP10-2012-07) and a Proof-of-Concept grant (NRF2015NRF-POC0001-19), the National Research Foundation of Korea (NRF) grant funded by the Korean Government (MSIT) (No. 2020R1C1C1004385), and the Ministry of Education, Youth and Sports grant LL2002 under the ERC CZ program. In addition, this work was supported by the Brain Pool Program through the National Research Foundation of Korea (NRF) funded by the Ministry of Science and ICT (2019H1D3A1A01070318). Further support was provided by the Singapore Centre for Environmental Life Sciences Engineering, whose research is supported by the National Research Foundation Singapore, Ministry of Education, Nanyang Technological University and National University of Singapore, under its Research Centre of Excellence Programme. Schematic illustrations were created with BioRender.com under an academic lab subscription.

Conflict of Interest

The authors declare no conflict of interest.

Data Availability Statement

Research data are not shared.

Keywords

bacterias, graphene oxide, nanomaterials, oxidative stress, surface functionalization

Received: March 9, 2021

Revised: March 22, 2021

Published online:

- [1] D. Wang, F. Peng, J. Li, Y. Qiao, Q. Li, X. Liu, *Mater. Today* **2017**, *20*, 238.
- [2] J. Li, W. Liu, X. Zhang, P. K. Chu, K. M. C. Cheung, K. W. K. Yeung, *Mater. Today* **2019**, *22*, 35.
- [3] Y. Wang, Y. Yang, Y. Shi, H. Song, C. Yu, *Adv. Mater.* **2020**, *32*, 1904106.
- [4] S. Kumari, G. Lang, E. DeSimone, C. Spengler, V. T. Trossmann, S. Lücker, M. Hudel, K. Jacobs, N. Krämer, T. Scheibel, *Mater. Today* **2020**, *41*, 21.
- [5] X. Hu, J. Tian, C. Li, H. Su, R. Qin, Y. Wang, X. Cao, P. Yang, *Adv. Mater.* **2020**, *32*, 2000128.
- [6] A. M. Maan, A. H. Hofman, W. M. de Vos, M. Kamperman, *Adv. Funct. Mater.* **2020**, *30*, 2000936.
- [7] A. Panáček, L. Kvítek, M. Směkalová, R. Večeřová, M. Kolář, M. Röderová, F. Dyčka, M. Šebela, R. Pucek, O. Tomanec, *Nat. Nanotechnol.* **2018**, *13*, 65.
- [8] J. W. Metch, N. D. Burrows, C. J. Murphy, A. Pruden, P. J. Vikesland, *Nat. Nanotechnol.* **2018**, *13*, 253.
- [9] D. P. Linklater, V. A. Baulin, S. Juodkazis, R. J. Crawford, P. Stoodley, E. P. Ivanova, *Nat. Rev. Microbiol.* **2020**, *19*, 8.
- [10] A. Avellan, M. Simonin, E. McGivney, N. Bossa, E. Spielman-Sun, J. D. Rocca, E. S. Bernhardt, N. K. Geitner, J. M. Unrine, M. R. Wiesner, *Nat. Nanotechnol.* **2018**, *13*, 1072.
- [11] P. J. Alvarez, C. K. Chan, M. Elimelech, N. J. Halas, D. Villagrán, *Nat. Nanotechnol.* **2018**, *13*, 634.
- [12] X. Chen, X. Zhu, S. He, L. Hu, Z. J. Ren, *Adv. Mater.* **2020**, *2001240*.
- [13] G. Sai-Anand, A. Sivanesan, M. R. Benzigar, G. Singh, A.-I. Gopalan, A. V. Baskar, H. Ilbeygi, K. Ramadass, V. Kambala, A. Vinu, *Bull. Chem. Soc. Jpn.* **2019**, *92*, 216.
- [14] S. Sharifi, S. Z. Vahed, E. Ahmadian, S. M. Dizaj, A. Eftekhari, R. Khalilov, M. Ahmadi, E. Hamidi-Asl, M. Labib, *Biosens. Bioelectron.* **2020**, *150*, 111933.
- [15] X. Zou, L. Zhang, Z. Wang, Y. Luo, *J. Am. Chem. Soc.* **2016**, *138*, 2064.
- [16] Q. Xin, H. Shah, A. Nawaz, W. Xie, M. Z. Akram, A. Batool, L. Tian, S. U. Jan, R. Boddula, B. Guo, *Adv. Mater.* **2019**, *31*, 1804838.
- [17] S. Liu, T. H. Zeng, M. Hofmann, E. Burcombe, J. Wei, R. Jiang, J. Kong, Y. Chen, *ACS Nano* **2011**, *5*, 6971.
- [18] O. N. Ruiz, K. S. Fernando, B. Wang, N. A. Brown, P. G. Luo, N. D. McNamara, M. Vangness, Y.-P. Sun, C. E. Bunker, *ACS Nano* **2011**, *5*, 8100.
- [19] I. Barbolina, C. Woods, N. Lozano, K. Kostarelos, K. Novoselov, I. Roberts, *2D Mater.* **2016**, *3*, 025025.
- [20] H. M. Hegab, A. ElMekawy, L. Zou, D. Mulcahy, C. P. Saint, M. Ginic-Markovic, *Carbon* **2016**, *105*, 362.
- [21] V. Palmieri, M. C. Lauriola, G. Ciasca, C. Conti, M. De Spirito, M. Papi, *Nanotechnology* **2017**, *28*, 152001.
- [22] V. Palmieri, F. Bugli, M. C. Lauriola, M. Cacaci, R. Torelli, G. Ciasca, C. Conti, M. Sanguinetti, M. Papi, M. De Spirito, *ACS Biomater. Sci. Eng.* **2017**, *3*, 619.
- [23] V. Georgakilas, J. N. Tiwari, K. C. Kemp, J. A. Perman, A. B. Bourlinos, K. S. Kim, R. Zboril, *Chem. Rev.* **2016**, *116*, 5464.
- [24] V. I. Lushchak, *Chem.-Biol. Interact.* **2014**, *224*, 164.

- [25] R. Gaupp, N. Ledala, G. A. Somerville, *Front. Cell. Infect. Microbiol.* **2012**, *2*, 33.
- [26] S. S. Grant, D. T. Hung, *Virulence* **2013**, *4*, 273.
- [27] B. Krismer, M. Liebeke, D. Janek, M. Nega, M. Rautenberg, G. Hornig, C. Unger, C. Weidenmaier, M. Lalk, A. Peschel, *PLoS Pathog.* **2014**, *10*, e1003862.
- [28] A. D. Potter, C. E. Butrico, C. A. Ford, J. M. Curry, I. A. Trenary, S. S. Tummarakota, A. S. Hendrix, J. D. Young, J. E. Cassat, *Proc. Natl. Acad. Sci. USA* **2020**, *117*, 12394.
- [29] K. L. Painter, E. Strange, J. Parkhill, K. B. Bamford, D. Armstrong-James, A. M. Edwards, *Infect. Immun.* **2015**, *83*, 1830.
- [30] S. E. Rowe, N. J. Wagner, L. Li, J. E. Beam, A. D. Wilkinson, L. C. Radlinski, Q. Zhang, E. A. Miao, B. P. Conlon, *Nat. Microbiol.* **2020**, *5*, 282.
- [31] C. K. Chua, Z. Sofer, M. Pumera, *Chem. - Eur. J.* **2012**, *18*, 13453.
- [32] L. Masip, K. Veeravalli, G. Georgiou, *Antioxid. Redox Signaling* **2006**, *8*, 753.
- [33] S. P. Watson, M. O. Clements, S. J. Foster, *J. Bacteriol.* **1998**, *180*, 1750.
- [34] M. Mortimer, N. Devarajan, D. Li, P. A. Holden, *ACS Nano* **2018**, *12*, 2728.
- [35] J. N. Belling, J. A. Jackman, S. Yorulmaz Avsar, J. H. Park, Y. Wang, M. G. Potroz, A. R. Ferhan, P. S. Weiss, N.-J. Cho, *ACS Nano* **2016**, *10*, 10161.
- [36] I. R. Booth, G. P. Ferguson, S. Miller, C. Li, B. Gunasekera, S. Kinghorn, *Biochem. Soc. Trans.* **2003**, *31*, 1406.
- [37] G. P. Ferguson, S. Töttemeyer, M. MacLean, I. R. Booth, *Arch. Microbiol.* **1998**, *170*, 209.
- [38] L. M. G. Bui, P. Hoffmann, J. D. Turnidge, P. S. Zilm, S. P. Kidd, *Infect. Immun.* **2015**, *83*, 470.
- [39] C. Lee, C. Park, *Int. J. Mol. Sci.* **2017**, *18*, 169.
- [40] P. Giesbrecht, T. Kersten, H. Maidhof, J. Wecke, *Microbiol. Mol. Biol. Rev.* **1998**, *62*, 1371.
- [41] K. C. Rice, K. W. Bayles, *Microbiol. Mol. Biol. Rev.* **2008**, *72*, 85.
- [42] A. A. Petti, C. A. Crutchfield, J. D. Rabinowitz, D. Botstein, *Proc. Natl. Acad. Sci. USA* **2011**, *108*, E1089.
- [43] U. Suttisansanee, J. F. Honek, *Semin. Cell Dev. Biol.* **2011**, *22*, 285.